

Syntheses, Structural Characterization, and Properties of Mn(II) and Cd(II) Complexes from 5-[4-(1H-Imidazol-1-Yl)phenyl]-1H-Tetrazole¹

H. W. Kuai^{a,*}, J. J. Xia^b, D. H. Li^a, T. Hu^a, and D. Y. Jiang^a

^aFaculty of Chemical Engineering, Huaiyin Institute of Technology, Huai'an, 223003 P.R. China

^bKey Laboratory for Traffic and Transportation Security of Jiangsu Province, Huaiyin Institute of Technology, Huai'an, 223003 P.R. China

*e-mail: hyitshy@126.com

Received June 20, 2016

Abstract—Reactions of Mn(II) and Cd(II) salts with 5-(4-(1H-imidazol-1-yl)phenyl)-1H-tetrazole (HL) under hydrothermal conditions result in complexes $[\text{Mn}(\text{L})_2(\text{H}_2\text{O})_4] \cdot 2\text{H}_2\text{O}$ (**I**) and $[\text{Cd}(\text{L})_2(\text{H}_2\text{O})_2]$ (**II**), which have been characterized by single crystal and powder X-ray diffractions (CIF files CCDC nos. 943861 (**I**), 943862 (**II**)), IR spectroscopy, element and thermogravimetric analyses. Two complexes exhibit structural diversity dependent on different metal salts. Complex **I** shows discrete mononuclear structure, which can be further linked to build a 3D supramolecular framework through hydrogen bonding interactions. Complex **II** displays 1D zigzag-chain structure, and an extended 3D framework can be formed by hydrogen bonding. Interestingly, tetranuclear water clusters were generated in **I**, which can be linked by Mn^{2+} ions to show 1D metal-bridged water cluster-chain structure. The present work provides an example that metal centers impact on coordination modes of ligand and consequent structural variation of resulted complexes. Moreover, fluorescence property of **II** was investigated.

Keywords: Mn(II) and Cd(II), structural characterization, water cluster, fluorescence

DOI: 10.1134/S1070328417070065

INTRODUCTION

Recently, coordination supramolecular chemistry is mainly concerned with the design and assembly of new crystalline materials with interesting properties and potential applications in many fields [1]. Consequently, exploration of such inorganic-organic hybrid materials has gradually become the main aim of crystal engineering [2]. It is known that functional properties of complexes are largely dependent on the nature of the metal centers and bridging ligands, and their architectures [3]. Meanwhile, many influential factors can impact on the structures of complexes. This may also supply feasibility to composite complexes with novel multifunctional properties and allow access to a vast domain of potentially multifunctional materials via attempting different synthetic conditions to achieve structural variation [4]. Among many influential factors, the intrinsic nature of organic ligands has been documented as crucial roles in the formation of coordination supramolecular compounds, which stimulate an impetus to select versatile ligands for exploration of new crystalline materials and new

insight into the correlation between synthetic conditions and the structure of resulted complexes [5].

We have recently carried out a study on synthesizing complexes under different experimental conditions based on 5-(4-(1H-imidazol-1-yl)phenyl)-1H-tetrazole (HL) ligand. As a mixed N-donor ligand, namely tetrazolyl and imidazolyl coordination groups, the HL may be a competent candidate for formation of complexes due to its fine coordinating capacities and variable coordination modes [6]. Compared with other N-donor ligand, the HL possesses several remarkable features as follows: (1) its rigid skeleton can reduce the coordination uncertainty and may favor to assemble polymers with high stability; (2) five potential coordination sites in the HL ligand endow it a peculiar characteristic to adopt variable coordination modes to satisfy geometric requirement of metal centers. Therefore, the HL ligand can be expected to induce new coordination insight for structural evolution of complexes.

In our previous work, we employed different transition metal salts to react with HL and polycarboxylate auxiliary co-ligands, such as terephthalic acid and obtained Co(II) and Zn(II) complexes, the structural diversity of which is dependent on the metal salts [7].

¹ The article is published in the original.

As an extension of previous research work, we used more transition metal salts to react with the HL ligand for further investigating correlation between synthetic conditions and structures of complexes. The structures of $[\text{Mn}(\text{L})_2(\text{H}_2\text{O})_4] \cdot 2\text{H}_2\text{O}$ (**I**) and $[\text{Cd}(\text{L})_2(\text{H}_2\text{O})_2]$ (**II**) have previously been reported as short communications [8]. However, we herein present further detailed syntheses, fully structural characterization, and fluorescent properties of **I** and **II**.

EXPERIMENTAL

Materials and methods. All commercially available chemicals were of reagent grade and used as received without further purification. According to the reported literature [9], a slightly revised experimental procedure was used to synthesize the HL ligand. Elemental analyses of C, H, and N were taken on a Perkin-Elmer 240C elemental analyzer. IR spectra were recorded on a Bruker Vector22 FT-IR spectrophotometer by using KBr pellets. Thermogravimetric (TG) analysis was performed on a simultaneous SDT 2960 thermal analyzer under nitrogen atmosphere with a heating rate of 10 K min^{-1} . The luminescence spectra for the powdered solid samples were measured on an Aminco Bowman Series 2 spectrofluorometer with a xenon arc lamp as the light source. In the measurements of emission and excitation spectra the pass width was 5 nm, and all measurements were carried out under the same experimental conditions.

Synthesis of I. A solution of $\text{MnCl}_2 \cdot 4\text{H}_2\text{O}$ (19.8 mg, 0.1 mmol), HL (42.4 mg, 0.2 mmol), and KOH (11.2 mg, 0.2 mmol) in 10 mL H_2O was stirred for 30 min. Then reaction mixture was placed in a 16 mL Teflon-lined stainless steel container and heated at 180°C for 48 h. And then the oven was shut off and cooled down naturally at ambient temperature. After cooling to the room temperature, colorless block crystals of **I** were obtained with an approximate yield of 45% based on the HL.

For $\text{C}_{20}\text{H}_{26}\text{N}_{12}\text{O}_6\text{Mn}$ ($M = 585.47$)

anal. calcd., %: C, 41.03; H, 4.48; N, 28.71.
Found, %: C, 41.31; H, 4.70; N, 28.66.

IR data (ν , cm^{-1}): 3320 $\nu(\text{C}-\text{N})$, 1618 $\nu(\text{C}=\text{N})$, 1309 $\nu(\text{C}-\text{N})$.

Synthesis of II. Reaction mixture of CdCl_2 (18.3 mg, 0.1 mmol), HL (42.4 mg, 0.2 mmol), and KOH (11.2 mg, 0.2 mmol) in 10 mL H_2O was sealed in a 16 mL Teflon-lined stainless steel container and heated at 180°C for 72 h. Then the oven cooled down at the rate of 10 K/h. After cooling to the room tem-

perature, colorless slender crystals of **II** were obtained with an approximate yield of 40% based on HL.

For $\text{C}_{20}\text{H}_{18}\text{N}_{12}\text{O}_2\text{Cd}$ ($M = 570.86$)

anal. calcd., %: C, 42.08; H, 3.18; N, 29.44.
Found, %: C, 42.32; H, 2.89; N, 29.22.

IR data (ν , cm^{-1}): 3362 $\nu(\text{C}-\text{N})$, 1669 $\nu(\text{C}=\text{N})$, 1329 $\nu(\text{C}-\text{N})$.

X-ray structure determination. The crystallographic data collections for complexes **I** and **II** were carried out on a Bruker Smart Apex II CCD area-detector diffractometer using graphite-monochromated MoK_α radiation ($\lambda = 0.71073\text{ \AA}$) at $293(2)\text{ K}$. The diffraction data were integrated by using the program SAINT [10], which was also used for the intensity corrections for Lorentz and polarization effects. Semi-empirical absorption corrections were applied using the program SADABS [11]. The structures of **I** and **II** were solved by direct methods, and all non-hydrogen atoms were refined anisotropically on F^2 by the full-matrix least squares technique using the SHELXL-97 crystallographic software package [12]. In **I** and **II**, all hydrogen atoms in C atoms were generated geometrically, while the hydrogen atoms in water could be found at reasonable positions in the difference Fourier maps and located there. The details of crystal parameters, data collection, and refinements are summarized in Table 1; the selected bond lengths and angles are listed in Table 2.

Supplementary material for structures has been deposited with the Cambridge Crystallographic Data Centre (CCDC nos. 943861 (**I**), 943862 (**II**); deposit@ccdc.cam.ac.uk or http://www.ccdc.cam.ac.uk/data_request/cif).

RESULTS AND DISCUSSION

The hydrothermal reactions of stoichiometric amounts Mn(II) and Cd(II) salts with HL at 180°C in the presence of KOH as alkaline reagent for the deprotonation can yield complex **I** and **II**. Complexes **I** and **II** are stable in air.

Complex **I** was obtained by hydrothermal reaction of $\text{MnCl}_2 \cdot 4\text{H}_2\text{O}$ and HL in the presence of KOH in a Teflon-lined reactor at 180°C . Single crystal consists of neutral $[\text{Mn}(\text{L})_2(\text{H}_2\text{O})_4]$ mononuclear entities and crystallization water molecules. The asymmetric unit of **I** contains one Mn(II) with 0.5 site occupancy, one L⁻ ligand, two coordinated water and one lattice water molecules. As shown in Fig. 1a with an atom numbering scheme, Mn(II) is located on a two-fold rotation axis and has a distorted octahedral coordination geometry with N_2O_4 donor set from four water and two L⁻. The Mn–N and average Mn–O distance around Mn(II) are 2.261(4) and 2.195 Å, respectively. According to bond distances and angles, slight distortion of

Table 1. Crystallographic data and structure refinement for **I** and **II**

Parameter	Value	
	I	II
M_r	585.47	570.86
Crystal size, mm	$0.20 \times 0.20 \times 0.20$	$0.30 \times 0.05 \times 0.05$
Crystal system	Monoclinic	Triclinic
Space group	$C2/c$	$P\bar{1}$
$a, \text{\AA}$	19.2382(18)	7.6283(8)
$b, \text{\AA}$	13.1362(12)	8.0420(9)
$c, \text{\AA}$	13.410(2)	9.1827(10)
α, deg	90	102.6780(10)
β, deg	129.9420(10)	97.9620(10)
γ, deg	90	106.0350(10)
$V, \text{\AA}^3$	2598.3(6)	516.16(10)
Z	4	1
$\rho_{\text{calcd}}, \text{g cm}^{-3}$	1.50	1.84
$\mu(\text{Mo}K_{\alpha}), \text{cm}^{-1}$	0.57	1.1
$F(000)$	1212	286
Limiting indices hkl	$-22 \leq h \leq 16, -15 \leq k \leq 13, -15 \leq l \leq 15$	$-8 \leq h \leq 9, -9 \leq k \leq 9, -10 \leq l \leq 11$
Θ Range for data collection, deg	2.08–25.00	2.33–25.60
Reflection measured	6481	2760
Reflection unique	2291	1912
R_{int}	0.0622	0.0068
Parameters refined	165	160
GOOF (F^2)**	1.084	1.082
$R(F)/wR(F^2)$ ** (all data)	0.0799/0.2326	0.0213/0.0542
$R(F)/wR(F^2)$ ** ($I > 2\sigma(I)$)	0.0803/0.2376	0.0211/0.0541
$\Delta\rho_{\text{max}}/\Delta\rho_{\text{min}}, e \text{\AA}^{-3}$	1.51/–1.46	0.48/–0.42

* $R_1 = \Sigma |F_o| - |F_c| / \Sigma |F_o|$. ** $wR_2 = |\Sigma w(|F_o|^2 - |F_c|^2)| / |\Sigma w(F_o)^2|^{1/2}$, where $w = 1/[\sigma^2(F_o^2) + (aP)^2 + bP]$, $P = (F_o^2 + 2F_c^2)/3$.

the O_h symmetry structure takes place indeed, which might originate from Jahn–Teller effect based on the consideration of the possession of electronic degenerate ground state of high-spin Mn^{2+} ion with $d^5 [(t_{2g})^3(e_g)^2]$ electron configuration in the complex [13]. The L^- ligand acts as counterion in the complex after deprotonation of tetrazolyl group. In spite of containing five potential coordination sites, the L^- ligand in complex **I** adopts terminal monodentate mode: each imidazolyl group coordinates to a $\text{Mn}(\text{II})$ and tetrazolyl moiety is free of coordination. Compared with another manganese complex with the L^- ligand [14], complex **I** shows an analogous structure except

relative orientation of two $\text{Mn}–\text{N}$ bonds in the coordination geometry and the existence of lattice water.

Due to the presence of N and O atoms in the complex, the delicate hydrogen bonding interactions exist extensively in the complex and play a decisive role in regulating the resulting supramolecular framework. Discrete mononuclear entities can be further linked by $\text{O}–\text{H} \cdots \text{N}$ weak interactions to form an extended 2D network structure (Fig. 1b, Table 3). Interestingly, between adjacent layers coordinated and lattice water molecules are interconnected by $\text{O}–\text{H} \cdots \text{O}$ bonding interactions to generate tetranuclear water clusters (Fig. 1c), which can be linked by Mn^{2+} ions to show 1D metal-bridged water cluster-chain

Table 2. Selected bond lengths (Å) and angles (deg) for complexes **I** and **II***

Bond	<i>d</i> , Å	Bond	<i>d</i> , Å
I			
Mn(1)–O(1)	2.208(5)	Mn(1)–O(2)	2.184(5)
Mn(1)–N(11)	2.263(6)		
II			
Cd(1)–O(1)	2.4610(16)	Cd(1)–N(1)	2.2623(18)
Cd(1)–N(3) ^{#1}	2.383(2)		
Angle	ω , deg	Angle	ω , deg
I			
O(1)Mn(1)O(2)	80.80(19)	O(1)Mn(1)O(2) ^{#1}	91.06(18)
O(1)Mn(1)O(1) ^{#1}	168.75(15)	O(2)Mn(1)N(11)	168.5(2)
O(1)Mn(1)N(11) ^{#1}	99.84(17)	O(2)Mn(1)O(2) ^{#1}	87.74(18)
O(2)Mn(1)N(11) ^{#1}	90.23(19)	N(11)Mn(1)N(11) ^{#1}	94.0(2)
O(1)Mn(1)N(11)	87.88(18)		
II			
O(1)Cd(1)N(1)	94.72(6)	N(1)Cd(1)N(3) ^{#1}	90.35(7)
O(1)Cd(1)N(3) ^{#1}	81.76(6)		

* Symmetry transformations used to generate equivalent atoms: ^{#1} $-x, y, 1/2 - z$ (**I**); ^{#1} $-1 + x, -1 + y, -1 + z$ (**II**).

Table 3. Geometric parameters of hydrogen bonds for complexes **I** and **II***

D–H···A	<i>D</i> ···A, Å	Angle D–H···A, deg
I		
O(1)–H(8)···N(5) ^{#1}	2.844(9)	173
O(1)–H(9)···N(4) ^{#2}	2.822(6)	170
O(2)–H(10)···O(3) ^{#3}	2.692(8)	166
O(2)–H(11)···O(3)	2.751(6)	169
O(3)–H(12)···N(3) ^{#2}	2.758(6)	168
O(3)–H(12)···N(4) ^{#2}	3.392(6)	142
O(3)–H(13)···N(5) ^{#4}	3.313(6)	140
O(3)–H(13)···N(6) ^{#4}	2.792(7)	167
II		
O(1)–H(8)···N(5) ^{#1}	2.949(2)	175
O(1)–H(9)···N(6) ^{#2}	2.914(3)	175

* Symmetry transformations used to generate equivalent atoms: ^{#1} $1/2 - x, 1/2 - y, -z$; ^{#2} $x, y, 1 + z$; ^{#3} $-x, 1 - y, 1 - z$; ^{#4} $1/2 - x, 1/2 + y, 1/2 - z$ (**I**). ^{#1} $1 - x, 2 - y, 1 - z$; ^{#2} $x, -1 + y, -1 + z$ (**II**).

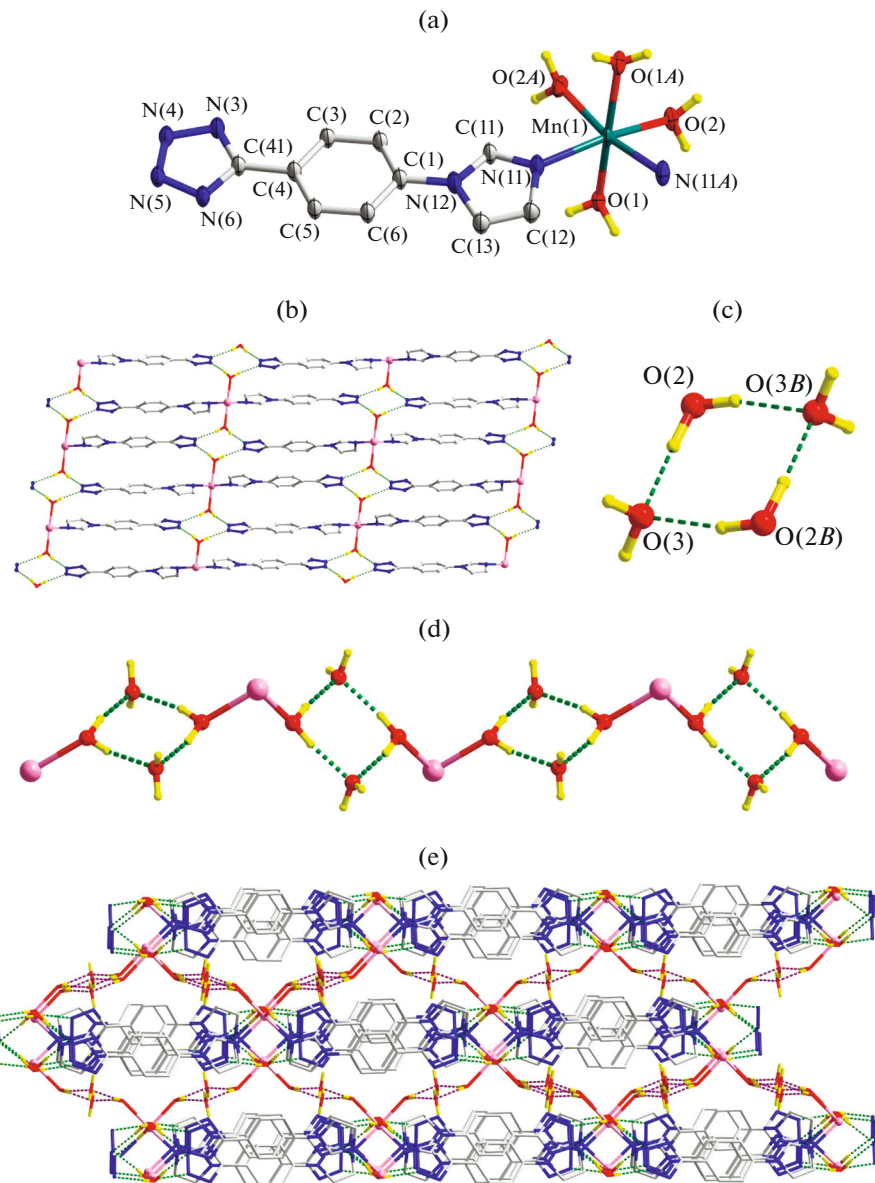


Fig. 1. The coordination environment of the Mn(II) in **I** with 30% probability displacement ellipsoids. Some hydrogen atoms and lattice water were omitted for clarity (a); 2D network of **I** extended by hydrogen bonds (b); view of four tetranuclear water cluster existing in **I** (c); view metal-bridged water cluster-chain structure (d); the extended 3D framework of **I** (e).

structure (Fig. 1d). Then adjacent layers are further bridged by the water clusters to construct a 3D supramolecular framework (Fig. 1e).

When CdCl₂ was introduced into hydrothermal reaction system as metal resource instead of MnCl₂ · 4H₂O, complex **II** was obtained, which displays 1D zigzag-chain structure. The asymmetric unit of **II** consists of one Cd(II) with 0.5 site occupancy, one L⁻ ligand, and one coordinated water. Each Cd(II) is located on an inversion center and six coordinated to

show a distorted octahedral coordination geometry with N₄O₂ donor set from two N_{imidazoly} atoms, two N_{tetrazoly} atoms, and two O_{water} atoms (Fig. 2a). From the perspective of crystallographic symmetry, the six coordinating atoms around Cd²⁺ ion can be grouped into two equivalent types, and consequently, the six coordinative bonds can equivalently be simplified into three pairs (Cd(1)–N(1) 2.2623(18), Cd(1)–N(3)^{#1} 2.3837(18), Cd(1)–O(1) 2.4609(16) Å). The bond distances and angles around Cd(II) can embody the

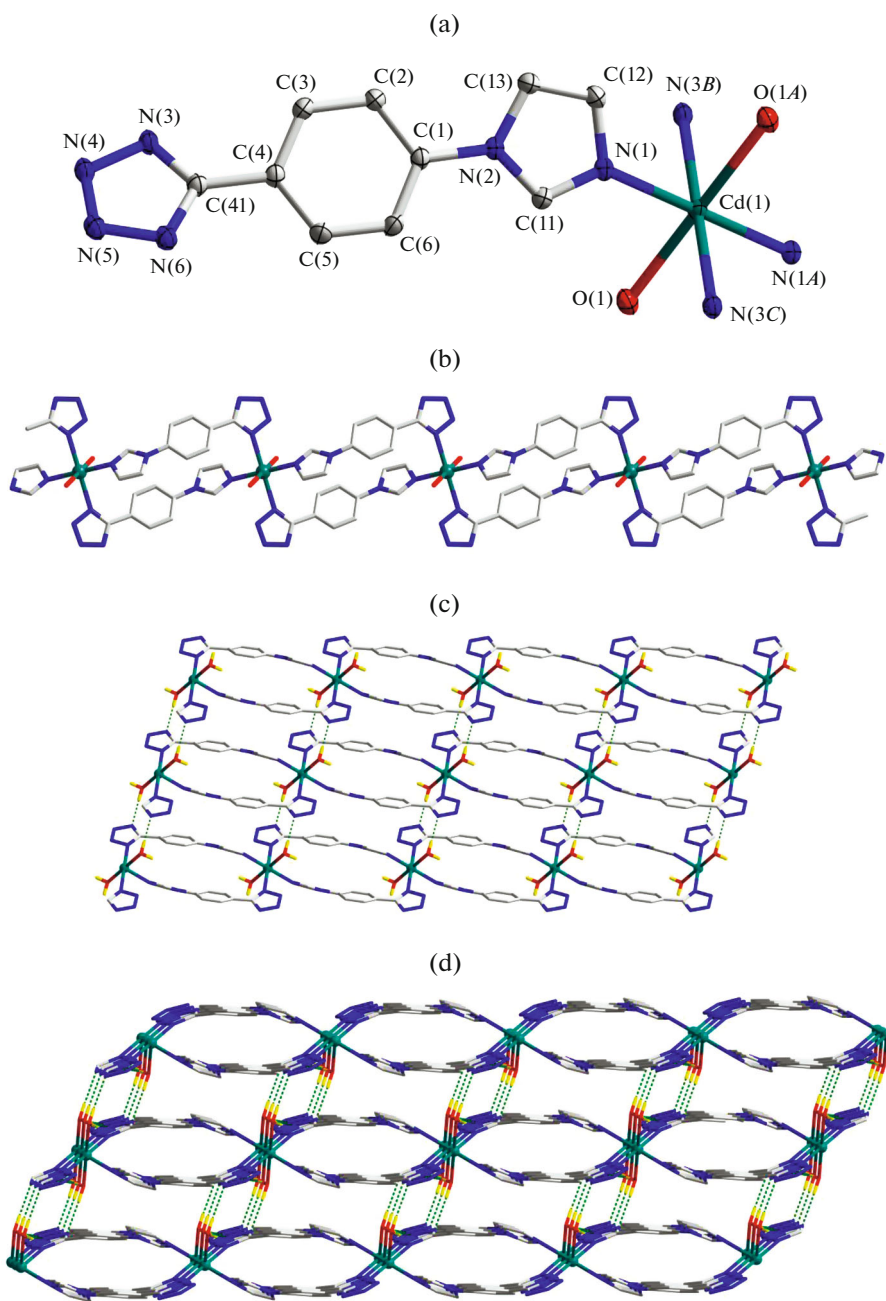


Fig. 2. The coordination environment of the Cd(II) in **II** with 30% probability displacement ellipsoids (hydrogen atoms were omitted for clarity) (a); view of 1D structure of **II** (b); view of 2D network of **II** extended by hydrogen bonds (c); the extended 3D framework of **II** (d).

almost standard octahedral coordination geometry with the O_h symmetry. Different from in complex **I**, the L^- ligand in **II** exhibits μ_2 -bidentate coordination mode: both imidazolyl and tetrazolyl groups coordinate to a single Cd²⁺ ion. Each Cd²⁺ ion is doubly interconnected by four L^- ligands, which repeats infinitely to yield a 1D zigzag-chain, within which

contains 22-membered uncoplanar metallacycles with intermetallic separations of Cd···Cd 11.02 Å (Fig. 2b). Adjacent chains can be further linked by O—H···O weak interactions to form a 2D network (Fig. 2c, Table 3), which can be bridged by the existing interactions to finally construct a 3D supramolecular framework (Fig. 2d).

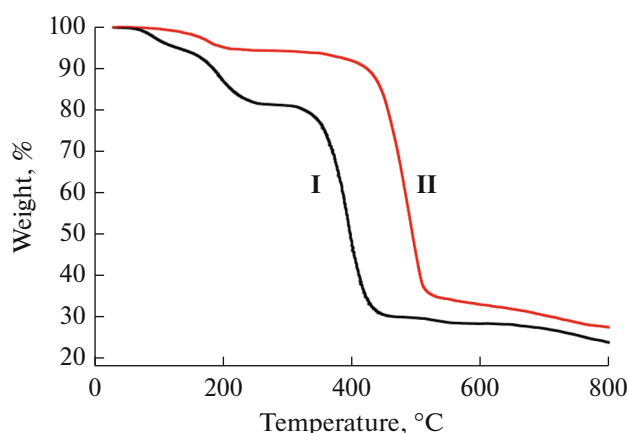
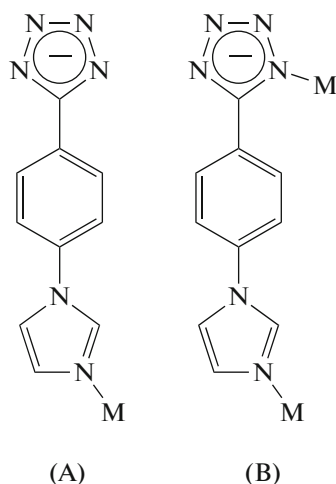


Fig. 3. The TGA curves of complexes **I** and **II**.

Complexes **I** and **II** were synthesized under the same synthetic conditions except different metal salts. Moreover, both Mn(II) and Cd(II) are six-coordinated showing octahedral coordination geometry. But **I** and **II** exhibit discrete mononuclear and 1D zigzag-chain structures, respectively. What lead to structural diversity of the complexes are different coordination modes of the L^- ligand: terminal monodentate and μ_2 -bidentate modes. The coordination modes of the L^- ligand in **I** (A) and **II** (B) are given in Scheme:



The present work provides an example that metal centers impact on coordination modes of ligand and consequent structural variation of resulted complexes.

The phase purity of complexes **I** and **II** could be proven by powder X-ray diffraction analyses. Each pattern of the bulk sample was in agreement with the simulated pattern from the corresponding single crystal data.

The TG were carried out for complexes **I** and **II** at N_2 atmosphere. The TG results are recorded from 30–800°C and shown in Fig. 3. Complex **I** shows continuous weight loss of 6.22% from 72 to 155°C corresponding to the release of lattice water (calcd. 6.15%)

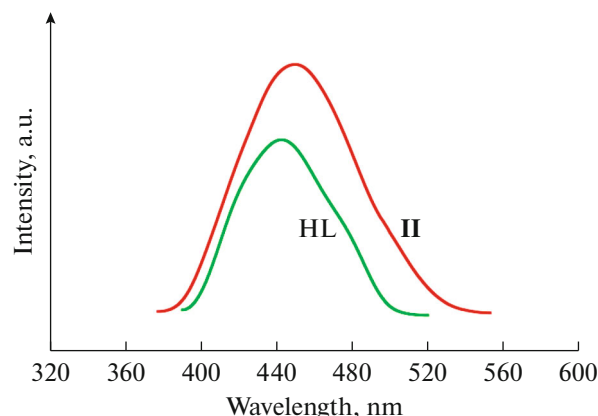


Fig. 4. Fluorescence of **II** and the HL ligand in the solid state at room temperature.

and a subsequent weight loss of 12.03% originating from the liberation of coordinated water (calcd. 12.30%). The decomposition of the framework of **I** begins at 313°C. For complex **II**, a weight loss of 6.02% from 115 to 210°C can be observed attributable to the coordinated water (calcd. 6.31%), and the decomposition of framework starts at 353°C.

Previous studies have revealed that coordination compounds containing d^{10} metal centers such as Cd(II) may exhibit excellent luminescent properties and have potential applications as photoactive materials [15, 16]. In the present work, luminescence of complex **II** and the HL has been investigated in the solid state at room temperature. As shown in Fig. 4, intensive fluorescent emission can be observed with emission bands at 450 nm ($\lambda_{ex} = 360$ nm) for **II** and 442 nm ($\lambda_{ex} = 370$ nm) for HL ligand. The fluorescent emission of **II** may be tentatively assigned to intra-ligand transition of coordinated L^- ligands, since similar emission was observed for free HL [15, 16]. The observation of red shift of the emission maximum in complex **II** compared with free HL ligand may originate from the coordination of the ligands to the metal centers [17, 18].

ACKNOWLEDGMENTS

The authors thank Natural Science Foundation for Universities in Jiangsu Province (16KJB150005) and Huaiyin Institute of Technology (15HGZ006 and 491713325) for financial support of this work.

REFERENCES

1. Kuai, H.W., Xia, J.J., and Sang, H.Y., *Inorg. Chem. Commun.*, 2016, vol. 72, p. 73.
2. Kuai, H.W., Cheng, X.C., Li, D.H., et al., *J. Solid State Chem.*, 2015, vol. 228, p. 65.
3. Zhao, D., Liu, X.H., Shi, Z.Z., et al., *Dalton Trans.*, 2016, vol. 45, no. 36, p. 14184.

4. Cui, P.P., Zhao, Y., Lv, G.C., et al., *CrystEngComm*, 2014, vol. 15, no. 16, p. 6300.
5. Su, Z., Chen, M., Okamura, T.A., et al., *Inorg. Chem.*, 2011, vol. 50, no. 3, p. 985.
6. Chen, M.S., Chen, M., Takamizawa, S., et al., *Chem. Commun.*, 2011, vol. 15, no. 47, p. 3787.
7. Kuai, H.W., Cheng, X.C., and Zhu, X.H., *Inorg. Chem. Commun.*, 2012, vol. 25, no. 11, p. 43.
8. Wang, X., Yan, S.W., Chang, S.C., et al., *Acta Crystallogr., Sect. E: Struct. Rep. Online*, 2012, vol. 68, no. 4, p. m413.
9. Bauer, C.A., Timofeeva, T.V., Settersten, T.B., et al., *J. Am. Chem. Soc.*, 2007, vol. 129, no. 22, p. 7136.
10. *SAINT, Program for Data Extraction and Reduction*, Madison: Bruker AXS, Inc., 2001.
11. Sheldrick, G.M., *SADABS, Program for Bruker Area Detector Absorption Correction*, Göttingen: Univ. of Göttingen, 1997.
12. Sheldrick, G.M., *SHELXS/L-97, Programs for the Determination of Crystal Structure*, Göttingen: Univ. of Göttingen, 1997.
13. Kuai, H.W., Cheng, X.C., Feng, L.D., et al., *Z. Anorg. Allg. Chem.*, 2011, vol. 637, no. 11, p. 1560.
14. Cheng, X.C., *Acta Crystallogr., Sect. E: Struct. Rep. Online*, 2011, vol. 67, no. 12, p. m1757.
15. Huang, Y.Q., Ding, B., Song, H.B., et al., *Chem. Commun.*, 2006, vol. 10, no. 47, p. 4906.
16. Valeur, B., *Molecular Fluorescence: Principles and Applications*, Weinheim: Wiley-VCH, 2002.
17. Wang, X.L., Bi, Y.F., Liu, G.C., et al., *CrystEngComm*, 2008, vol. 9, no. 10, p. 349.
18. Zhang, L., Li, Z.J., and Lin, Q.P., *Inorg. Chem.*, 2009, vol. 48, no. 14, p. 6517.